Arsenic termination of the Si(110) surface

D. K. Biegelsen, R. D. Bringans, J. E. Northrup, M. C. Schabel, and L.-E. Swartz
Xerox Palo Alto Research Center, 3333 Coyote Hill Road, Palo Alto, California 94304
(Received 17 June 1992; revised manuscript received 11 November 1992)

Si(100) and Si(111) surfaces both have singly occupied dangling bonds in their lowest-energy configurations. A single monolayer of arsenic has been shown to passivate the surfaces and lead to simple, nearly ideal (2×1) and (1×1) reconstructions, respectively. The bare Si(110) surface also has a complex reconstruction and high surface free energy. As presented here it can be shown theoretically that termination of Si(110) with a monolayer of As lowers the free energy of the ideal surface by 1.1 eV/(As atom). We would therefore expect that As adsorption would again lead to a topographically simple passivated structure. Using x-ray-photoemission spectroscopy, low-energy electron diffraction, and scanning tunneling microscopy we show here that, to the contrary the Si(110):As surface, in fact consists of $\frac{2}{3}$ monolayer of As in a two-dimensional corrugated unit cell with real-space unit vectors 5α and $3\alpha+3\beta$, where $\alpha=[001]$ and $\beta=\frac{1}{2}[1\text{–}10]$. We propose a model for the surface which consists only of fourfold-coordinated Si atoms and threefold-coordinated As atoms.

I. INTRODUCTION

An ideally truncated Si surface has dangling bonds (DB's) with energy levels lying within the surface band gap. Bare Si is therefore very reactive. The higher formation energy of the ideal surface leads to reconstructions, which lower the energy by reducing the DB densities. The Si(111)7×7 reconstruction is the best known example. An image obtained by scanning tunneling microscopy (STM) is shown in Fig. 1(a). There stacking faults, dimerization, and adatom capping are utilized to reduce the DB density from 1 per surface atom to ~0.4/atom.[1] Arsenic has been shown to passivate the Si(111) and Si(100) surfaces.[2] Complete surface rearrangement can occur (in reasonable times) at temperatures as low as 300 °C. The doubly occupied As dangling bond (or lone pair) at the surface has an energy that is degenerate with the top of the valence band. The free energy is therefore very low and the surface is extremely nonreactive. When As_4 is incident on a bare Si surface, even at room temperature, the molecules are cracked at the Si surface and chemisorption is induced. Figure 1(b) shows a Si(111) surface terminated by one monolayer (ML) of As. A simple 1×1 structure is now observed. Arsenic termination occurs, in less striking contrast, for Si(100) surfaces. There also the passivation saturates at 1 ML coverage. We point out here though that termination by P,[3] Sb,[4] or Bi,[5] instead of As, leads to a much more disordered and/or more complex surface reconstruction on both Si(111) and Si(100) surfaces. Atomic size and strain therefore are quite important in allowing the Si:As passivation to occur simply and completely.

The bare Si(110) surface is known to have one or more very complex reconstructions[6] and is often dominated by low levels of impurities.[7] However, with the above results for Si(111) and Si(100) in mind, we expected the Si(100):As surface to consist of a monolayer of As in a relaxed ideal 1×1 lattice termination with no reconstruction, or to form As-terminated (111) microfacets. These structures would leave all As atoms threefold coordinated and all Si atoms fourfold coordinated.

The ideal Si(110) surface is shown in Fig. 2(a). The unit cell is spanned by basis vectors $\alpha=(001)$ and $\beta=\frac{1}{2}(1-10)$. In reality, clean Si(110) surfaces, free of metal contamination, order in stripes approximately 30 Å wide and alternating in height by one atomic layer.[7] The resulting large unit cell has basis vectors $a=\alpha+17\beta$ and $b=2\alpha+2\beta$. (This ordering has sometimes been given the misnomer of the "16×2" reconstruction.) Metallic contamination at levels as small as 10^{-2} ML has been shown to destroy the long-range order and introduce other reconstructions, characterized generally by rectangular 5× unit cells with axes parallel to α and β.[7]

II. EXPERIMENTAL RESULTS

Samples 5×18 mm were cut from polished, nominally on axis, 50-mm wafers. The material was boron doped with a resistivity of 10^{-2} Ω cm. In some cases, the polished surfaces were etched to remove residual metallic impurities from the commercial polishing process. After solvent cleans, HF dipping and mounting in molybdenum sample holders (using molybdenum bolts and tungsten wire clips to minimize metallic contamination), a thin suboxide was formed in the samples by the uv-ozone method.[8] After loading into an ultrahigh vacuum (UHV), samples were prebaked at 600 °C for several hours typically, then deoxidized and annealed at 1030 °C. At this stage, the low-energy electron-diffraction (LEED) pattern for as-polished samples was a complicated superposition of reconstructions. The polish etched samples showed the clean "16×2" LEED pattern. In no case did x-ray-photoemission spectroscopy (XPS) show any observable levels of contamination. Both types of samples were given a variety of As_4 exposures and thermal cycles and reobserved by LEED. (Recipes included slow cooling in an As_4 flux after oxide desorption, As termination starting at room temperature and thermally cycling to

650 °C and introducing As to the clean Si surface at 600 °C.) In all cases, the LEED patterns were almost identical and similar to that shown for example in Fig. 2(b) for $E=44$ eV. Trace impurities thus play no observable role in driving the reconstruction of the As-terminated Si(110) surface. This is, of course, quite plausible given the strong chemical bonding of As to Si and the concomitantly low surface formation energy. We further note that XPS measurements of the ratio of As $3d$ peak areas to Si $2p$ peak areas were independent of sample preparation method. The measured coverage was found to be 0.67 ± 0.05 ML (this error range is statistical and does not include possible systematic errors) when referenced to 1 ML for Si(100):As and accounting for the factor of $\sqrt{2}$ greater surface areal density on the (110) surface relative to the (100) surface. [The Si XPS intensity is independent of crystal orientation because the

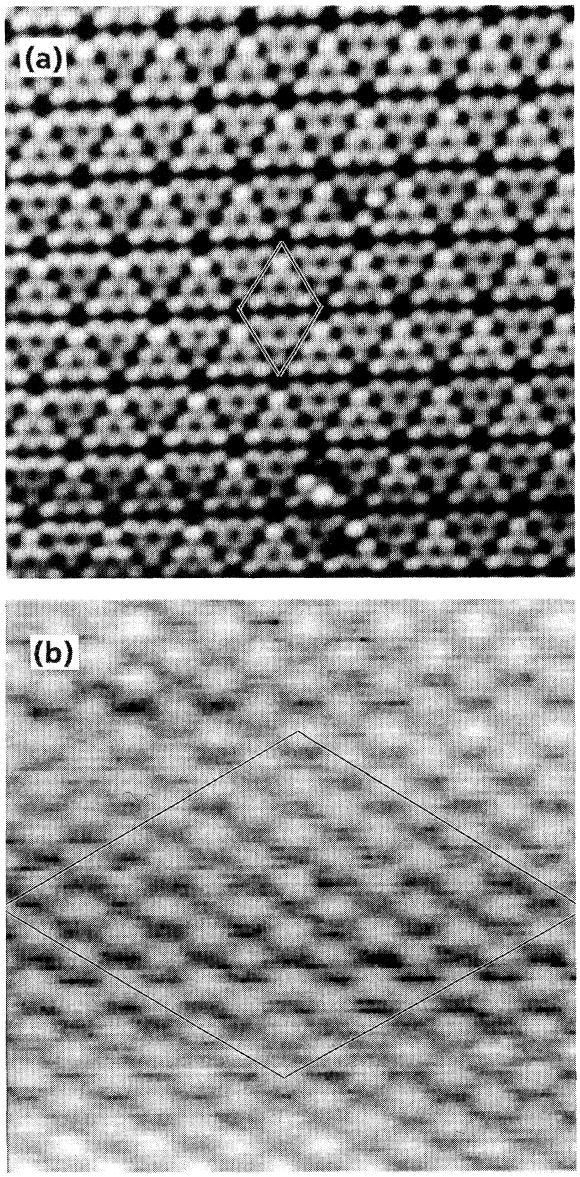

FIG. 1. Scanning tunneling microscope images of Si(111) surfaces. The sample bias was -2.0 V relative to the tip (filled states imaged) and demand current was 100 pA; (a) shows the (7×7) reconstruction of the bare surface and (b) shows the (1×1) As-terminated surface. Overlays indicate (7×7) cell size.

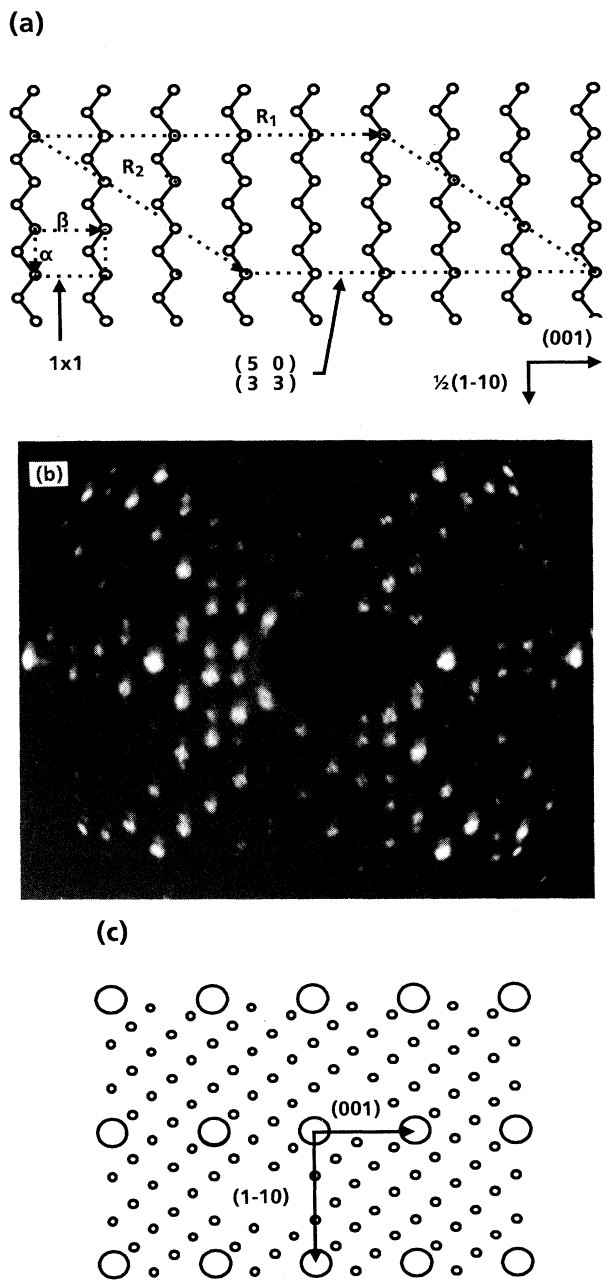

FIG. 2. (a) The ideally terminated Si(110) surface consisting of [1−10] chains of threefold-coordinated atoms. Overlays show a 1×1 cell for the ideal bare Si(110) surface and the real-space cell of the Si(110):As surface implied by the LEED results presented in (b) and (c); (b) LEED pattern from As-terminated Si(110) for $E=44$ eV; (c) inferred LEED spot pattern for single domain. Basis vectors are k-space conjugates corresponding to real-space directions [001] and [1−10].

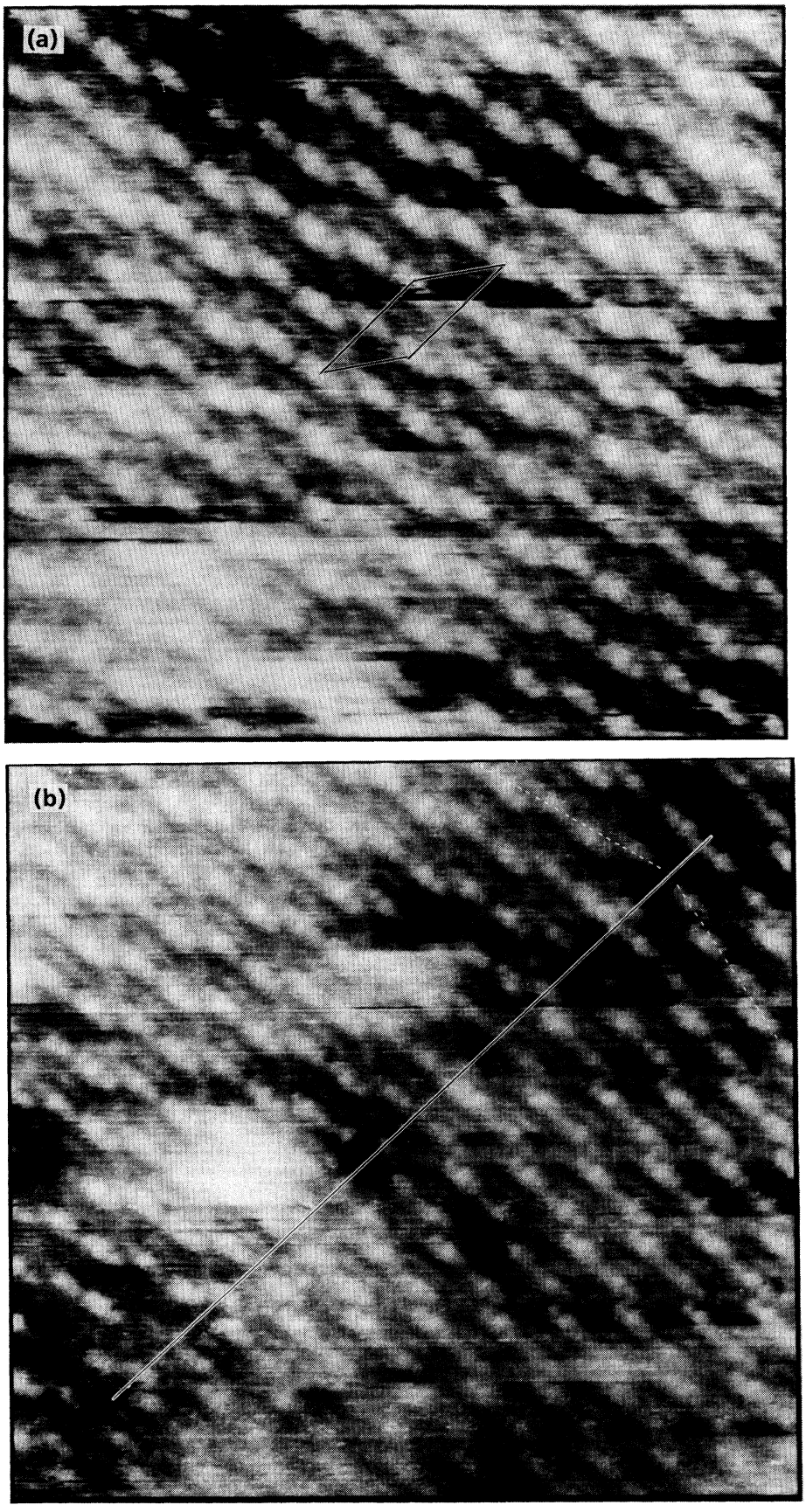

FIG. 3. STM images of Si(110) surface. Sample bias was −1.0 V relative to the tip. Demand current was 50 pA. (a) Typical gray scale image (where lightest represents highest above the surface) showing ordering of unit cells. Overlay indicates a unit cell as in Fig. 2(a). Image size is 16×16 nm. (b) Similar image including an antiphase reconstruction boundary. Image size is 18.5×18.5 nm.

effective probe volume includes the same number of bulk unit cells. In our definition, an As monolayer on the (110) surface corresponds to an areal density of As atoms which is a factor of $\sqrt{2}$ higher than an As monolayer on the (100) surface.]

The LEED structures are the superposition of two patterns arising from the two possible domains. In Fig. 2(c) we depict the deduced LEED spot pattern corresponding to a single domain. The inferred real-space net is shown in Fig. 2(a). One of the several equivalent, nonrectangular, real-space unit cells implied by the LEED analysis is spanned by basis vectors (5α) and $(3\alpha+3\beta)$—as drawn—and its twin, spanned by (5α) and $(3\alpha-3\beta)$.

To determine the internal structure of the complex unit cell, we used STM constant-current imaging at multiple bias voltages. The surfaces were found to be semiconducting. Figure 3(a) is a typical constant-current, gray scale topograph of filled electronic states showing the long-range ordering that is found. The image is unfiltered digitally and uncorrected for thermal drift and electromechanical skew. A unit cell consistent with that deduced from the LEED data is indicated by the superimposed lines. Figure 3(b) is a similar image of a region which includes parts of two antiphase domains. The

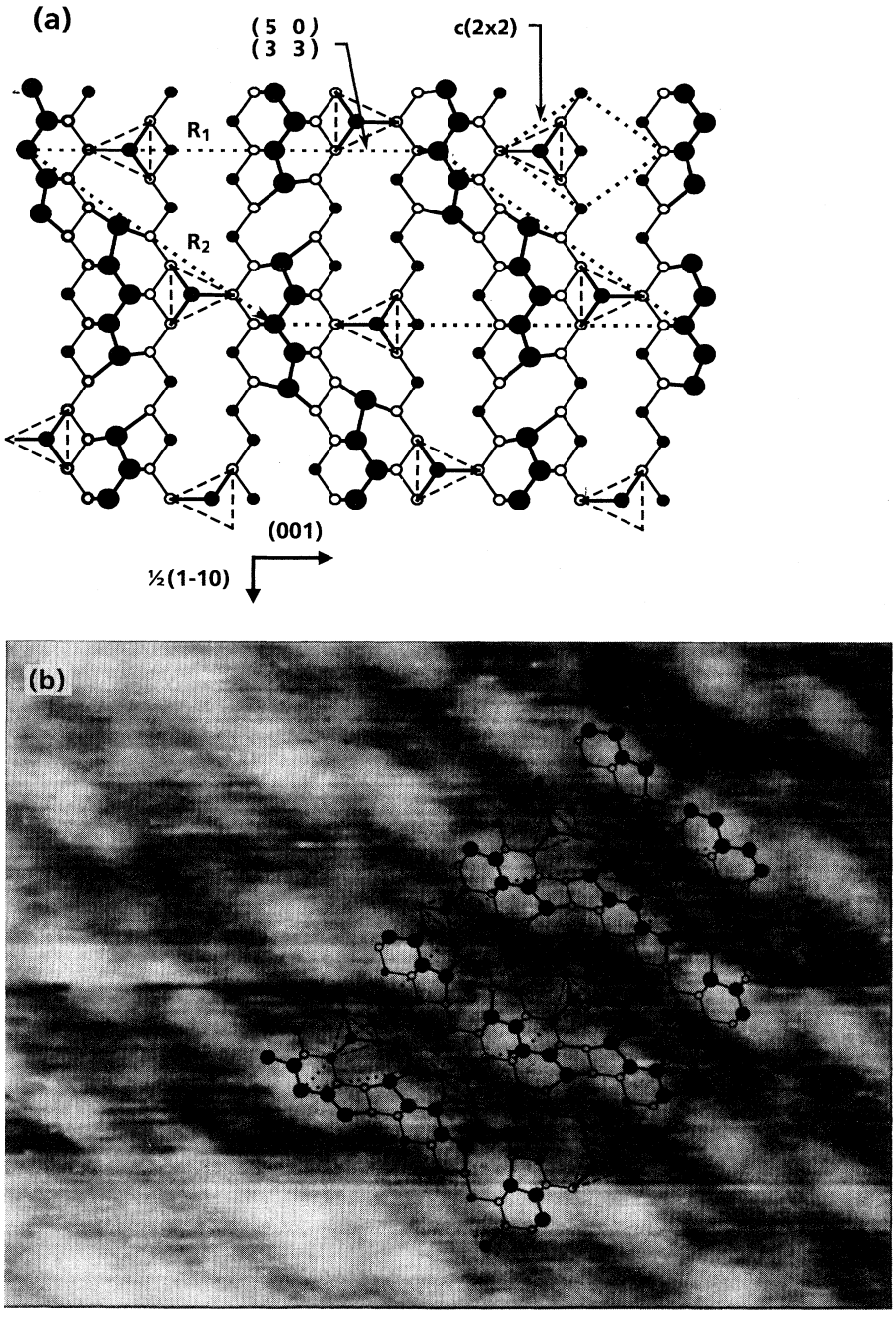

FIG. 4. (a) Ball and stick model of a $\frac{2}{3}$-ML As termination. Filled circles represent As atoms and empty circles represent Si. Largest filled circles lie in the top layer, intermediate sized circles represent the capping adatoms intermediate between layers, and the smallest filled circles represent substitutional As atoms in the lower layer. Dashed triangles are guides for the eye to mark adatom units. (b) Model superimposed on magnified region of Fig. 3(a). Image size is 6.5×8.5 nm.

overlaid line marks the mirrorlike twin boundary.

In simultaneously acquired pairs of filled- and empty-state images tip-retracted regions are found to be colocated. This implies that topographic structure is the primary cause of tip height variations in the constant current images. Line scans across monolayer steps (which run parallel to ⟨110⟩ directions) were used to calibrate the surface corrugation. The corrugation amplitude was found to be 0.7 ± 0.1 times the step height. This is an underestimate of the true unit-cell height range. Because the tip generally has a radius of curvature larger than half the valley width, the lowest point on the tip cannot follow the sample's isoelectronic state density contours to the valley minima. It is therefore quite plausible to conclude that the true surface structure has a two-layer corrugation. Also seen in the images are intensity modulated regions, both higher and lower, which have a characteristic size of approximately one unit cell. These always occur with opposite phases in filled- and empty-state image pairs. We therefore conclude that they are due to local band bending. The origin may be charged defects (e.g., kinks) or impurities. The density of charged centers is 10–100 times too high to arise from compensated substrate dopants if one assumes no surface segregation.

The images are of insufficient clarity to determine an atomic structure directly. [We have not been successful in obtaining better resolution. With the same system, atomic resolution on the less corrugated Si(100) and Si(111) surfaces, such as those shown in Fig. 1, is relatively easy to achieve—except at step edges. We surmise that the difficulty arises in large part from the corrugated nature of the surface. This enhances the broadening for all features due to surface topographic convolution with the tip.] Nevertheless, we have found only one kind of ball and stick model which reasonably replicates the STM features and has $\sim\frac{2}{3}$-ML coverage of As. An example is shown in Fig. 4(a) and overlaid in Fig. 4(b) on an enlarged area of Fig. 3(a). The consistently dominant features are broken chainlike sections parallel to (1–10) with a periodic structure of kinks. Parallel, lower-lying (1–10) features can also be observed between the upper linear segments. Finally one can ascertain localized features in the troughs positioned near the kinks and breaks. We tentatively ascribe these to threefold-coordinated capping As adatoms. The bare surface unit cell contains 30 Si atoms. Therefore a resulting occupation of 20 ± 1 As atoms would correspond to the coverage observed in XPS. The model presented has 22 As atoms per unit cell. (Adding one more As capping adatom, and therefore converting three As atoms in chains to Si atoms, would reduce the total to 20 As atoms per cell. However the 22-atom model fits better to the various STM images.) This type of model is chemically plausible in that all threefold sites are occupied by As atoms with doubly occupied lone pair orbitals and all Si atoms are fourfold coordinated. Furthermore, domain boundaries as shown in Fig. 3(b) are easily rationalized in terms of a relative shift in the chain jog direction.

III. THEORETICAL RESULTS

Realistic calculations for such complex unit cells are still beyond current computational capabilities. Nevertheless, several important points can be derived from theoretical considerations. Given the existence of topologically simple As-terminated reconstructions of the (111) and (100) faces, one expects that a similar situation exists for the (110) face. However, as discussed earlier, the fully saturated ideal topology Si(110):As 1×1 surface is not observed. We demonstrate by counter example that the ideal topology is also theoretically not the lowest energy (110) surface. Specifically, we show that a model containing As-terminated (111) microfacets is more stable. We argue that its greater stability follows from the exothermicity of the bond reaction Si-Si+As-As↔2 Si-As. We also present an estimate based on the Keating model of the surface stress tensor for the ideal surface.

TABLE I. Surface structures and stress calculated with the Keating model and density-functional theory (DFT). DFT results for the stresses (σ) on Si(100) and Si(111) surfaces are due to Meade and Vanderbilt, Ref. 16. Bond lengths are in Å and stresses in eV/(1×1 cell). For the (111) surface, a 1×1 cell has an area of $\sqrt{3a^2/2}$. For the (100) surface, the 1×1 cell area is a^2. For the (110) surface the 1×1 cell area is $\sqrt{2a^2}$ ($a=3.83$ Å).

			Si(111):As 1×1			
		$R_{\text{Si-As}}$	$\theta_{\text{As-Si-Si}}$			σ
Keating		2.425	104.7			2.27
DFT		2.42	105.0			2.27[a]
			Si(100):As 2×1			
	$R_{\text{Si-As}}$	$R_{\text{As-As}}$	$\theta_{\text{As-Si-Si}}$	$\theta_{\text{As-Si-As}}$	$\sigma_\perp$	$\sigma_\parallel$
Keating	2.42	2.69	105.0	100.1	2.05	2.56
DFT	2.43	2.50	104.6	102.4	2.35[a]	2.41[a]
			Si(110):As 1×1			
	$R_{\text{Si-As}}$	$R_{\text{As-As}}$	$\theta_{\text{Si-Si-As}}$	$\theta_{\text{As-Si-As}}$	$\theta_{\text{As-As-As}}$	$\sigma_\perp$	$\sigma_\parallel$
Keating	2.37	2.50	107.6	109.2	100.4	1.38	1.25
DFT	2.39	2.50	107.4	109.2	100.5		

[a]Reference 16.

The surface stress is found to be similar to the As-terminated (111) and (100) surfaces.

A. Surface energy

The surface energy for an As-terminated Si surface E_S is defined in terms of the quantity $\Omega = U - n_{Si}\mu_{Si(bulk)} - n_{As}\mu_{As}$, where $\mu_{Si(bulk)}$ is the chemical potential of bulk Si and μ_{As} is the chemical potential of the adsorbed As. U is the energy and/or cell of a periodic array of slabs modeling the As-terminated surfaces. The surface energy is defined here as $E_S = \Omega / N_S$, where N_S is the number of surface atoms. For the structures considered here, N_S is also equal to the number of As atoms (n_{As}). Thus, the *relative* values of the surface energies are independent of the chemical potential for As. The local-density approximation[9] and the first-principles pseudopotential method[10,11] were employed to calculate U. The calculations were carried out with a plane-wave basis with a kinetic-energy cutoff of 10 Ry. Atomic coordinates were determined via Hellmann-Feynman force calculations.

For As on Si(110), the simplest structure consists of one-dimensional chains of As atoms with each As atom bonded to one Si in the second layer and to two As atoms in the surface layer [similar to Fig. 2(a) with the surface Si atoms replaced by As atoms]. The calculated structural parameters are given in Table I. The calculated surface energies for the As-terminated surfaces are given in Table II for $\mu_{As} = \mu_{As(bulk)}$. Even though there are different numbers of Si-As and As-As bonds formed on these three surfaces, the surface energies are rather similar. The surface energies of the bare Si surfaces are in each case ~ 1 eV/(surface atom) higher than for the As-terminated surfaces. As adsorption on bare Si surfaces is energetically very favorable.

As one progresses from the (111) to the (100) to the (110) surface, the number of As-As bonds per As atom increases from 0 to 1 to 2, and the complementary number of Si-As bonds (per As atom) decreases from 3 to 2 to 1. The change in chemical bonding corresponds to the reaction Si-Si + As-As $\leftrightarrow$ 2 Si-As. The similarity in the values of E_S for the (111) and (110) surfaces implies that the energy gain in the bond reaction Si-Si + As-As $\leftrightarrow$ 2 Si-As is on the order of 0.1 eV. This reaction occurs once per As atom in a transformation from Si(110):As 1×1 to Si(111):As 1×1, and the surface energy is reduced by ~ 0.1 eV.[12] Moreover, simple bond counting arguments suggest that the energy of this bond reaction should be approximately equal to $\frac{2}{3}$ of the heat of formation of the compound SiAs. Recent calculation by Van de Walle[13] indicate a heat of formation of -0.12 eV for SiAs. Thus we conclude that such a bond reaction is exothermic (by ~ 0.1 eV) and that structural transformations which increase the number of *unstrained* Si-As bonds at the expense of Si-Si and As-As bonds may result in surfaces with lower formation energies. This could underlie the termination of As-As chains which is found on this surface.

TABLE II. Formation energies for singular silicon surfaces. The * denotes microfaceted (110)/{111}.

Structure		E_S (eV/As atom)	ΔE_S (eV/As atom)
Si(110)	1×1	1.40±0.1	
Si(110):As	1×1	0.27±0.1	1.13
Si(111)	1×1	1.46±0.1[a]	
Si(111):As	1×1	0.16±0.1	1.30
Si(100)	2×1	1.45±0.1[b]	
Si(100):As	2×1	0.38±0.1	1.07
Si(100):As	2×1*	0.17±0.1	

[a]Reference 17.
[b]Reference 18.

An interesting topological property of the Si(110) surface is that (111) oriented facets can form without increasing the number of threefold-coordinated surface atoms. Therefore, if $E_S(111) < E_S(110)$ the (110) surface will be unstable with respect to (111) facet formation. Our results indicate that the surface energy for Si(111):As is 0.11 eV/(As atom) lower than that for the Si(110):As 1×1 surface. This result suggests that models for the As-terminated (110) surfaces which consist of a mixture of (110) and (111) microfacets will be lower in energy than the ideal (110) surface. An example of such a microfacet model with a 2×1 periodicity is illustrated schematically in Fig. 5. This type of microfacet structure can be generalized to $n\times1$ periodicities in an obvious manner. The calculated surface energy of the 2×1 microfacet model was found to be 0.17 eV/(As atom). Thus the 2×1 surface is 0.1 eV/(As atom) more stable than the ideal Si(110):As 1×1 surface. Therefore, we conclude that the *ideal (110) As-terminated surface is not thermodynamically stable.* So although the ideal topology As-terminated surface has a low surface energy, at least one example of a morphologically more complex surface lies lower. In Fig. 6 we plot the surface formation energy versus As chemical potential. The slopes of the ideal and faceted Si(110):As surfaces are the same because each has the same number of As atoms per unit area.

B. Surface stress

The possibility that surface stress is an important factor in the destabilization of the Si(110):As 1×1 surface

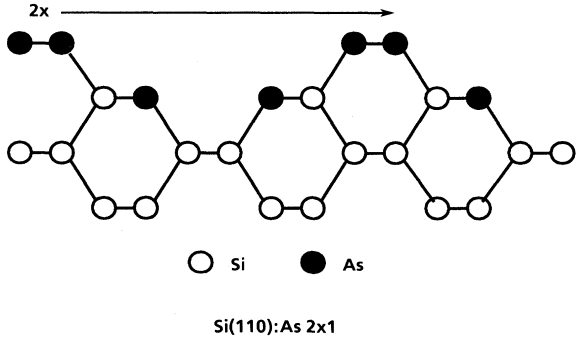

FIG. 5. Microfacet model of the Si(110) surface.

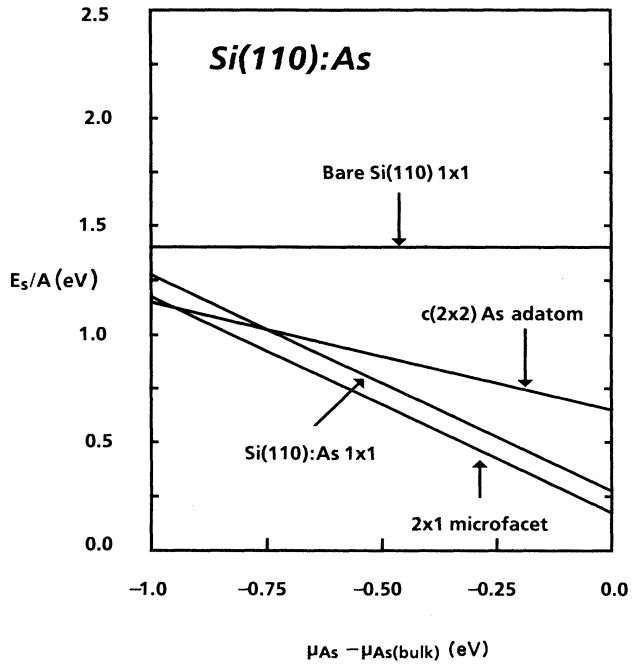

FIG. 6. Surface formation energy per atom for the bare Si(110), the Si(110):As flat, corrugated structures covered by 1-ML As and a $c(2\times2)$ adatom structure covered by $\frac{1}{2}$-ML As.

was investigated using a modified Keating[14] model. The form of the Keating potential is

$$U=\sum(3\alpha_{ij}/8R_{ij}^2)(\mathbf{r}_{ij}\cdot\mathbf{r}_{ij}-R_{ij}^2)^2 + \sum(3\beta_{ijk}/8R_{ij}R_{ik})(\mathbf{r}_{ij}\cdot\mathbf{r}_{ik}-R_{ij}R_{ik}\cos\theta_{ijk})^2 ,$$

where θ_{ijk} is the preferred bond angle for the $\langle ijk \rangle$ triplet of atoms. Surface atom rehybridization is accommodated within this model by allowing θ_{ijk} to vary from the tetrahedral value,[15] thus enabling reasonable simulation of a variety of As-terminated Si surfaces. Arsenic tends to prefer 90° bond angles due to the s^2p^3 hybridization and so this was the value chosen for the triplets having As at the vertex. R_{ij} is the optimal bond length between atoms i and j, and α_{ij} is the associated bond stretching force constant. β_{ijk} is the bond bending force constant for the $\langle ijk \rangle$ triplet. To determine the Keating bond stretching and bending parameters for the Si-As bond, we fixed the equilibrium Si-As bond length at 2.38 Å and then determined the geometry and surface stress for the Si(111)1×1:As surface over an extensive region of the parameter space. These data were then fitted using least squares to *ab initio* structural and stress data[16] for the same surface to obtain an optimal parameter set. Parameters for the As-As bond were then determined by calculating the geometry of the Si(110)1×1:As surface and using least squares to obtain the best fit to this structure. The resulting parameter set is given in Table III. The stresses and structures obtained with this set are compared with the *ab initio* results in Table I. Clearly, the stresses obtained with the Keating model agree well with those determined from density-functional calculations. In addition, these results are relatively insensitive to variation in the model parameters, indicating that the fitting procedure is stable. The surface stresses and structures for Si(100)2×1:As were calculated using the same parameter set, and show reasonable agreement for both the geometry and stresses despite the highly strained reconstruction of this surface. Therefore, since the surface stresses for the Si(111):As and Si(100):As surfaces are given accurately by the model, we expect that the predicted stresses for the Si(110):As 1×1 surface are also reasonably accurate. The significantly smaller values of $\sigma_\perp$ and $\sigma_\parallel$ (the stresses perpendicular and parallel to the As-As-As chains) for the (110) surface compared to the stresses on the (111) and (100) surfaces lead us to surmise that surface stress is not a significant driving force for the observed reconstruction of Si(110):As. In fact, we find that the surface stress for the 2×1 microfacet model is larger than the surface stress for the ideal 1×1 structure even though the former has a lower surface energy.

C. Energetic considerations of the experimental model

The structure observed in the present set of experiments has significantly less than one monolayer As coverage and is much more complicated than the ideal surface or the (111) microfaceted surface. Although elements of the (111) microfaceted surface can be seen, the [1−10] chains have apparent breaks and jogs. In the ball and stick model we have also invoked two instances of a capping arsenic atom which spans two second-layer chains. This structure was chosen both to fit the STM data as well as to reduce the As coverage to nearly agree with the XPS data.

To probe the energetics of the adatom subunit, calculations were performed for a $c(2\times2)$ model indicated in Fig. 4(a), except that every corner atom is a fourfold-coordinated Si. There is one As adatom and one As substitutional atom in each unit cell. The surface energy for

TABLE III. Keating model parameters.

		Si-As	As-As	Si-Si		
	α(eV/Å^2)	2.809	1.560	3.027		
	R^0(Å)	2.380	2.505	2.352		
	As-Si-Si	As-As-As	Si-Si-Si	Si-Si-As	As-As-Si	
β(eV/Å^2)	0.983	0.493	0.863	0.921	0.696	

such a model was found to be higher than those obtained for the fully saturated surfaces. In Fig. 6 we have plotted the results for the $c(2\times2)$ As-adatom structure which represents the adatom building block in the more complex structure. The slope corresponds to a 50% coverage of As. The energy elevation is most likely due to the strained bonds of the adatom configuration. It is possible that the energy of the adatom configuration is lowered when embedded in the complex strain fields of the surrounding chain segments. The proposed model can then be thought of as interacting units of [1−10] chain segments of the microfaceted surface and As-adatom bridging units. Although this structure is not one we would have guessed based on physical intuition, its physical existence, independent of the details of sample preparation, implies an energetic minimization. The dominant energetic elements are still not understood. Currently, the size and complexity of the actually occurring cell precludes a first-principles calculation of the surface formation energy for comparison and analysis.

IV. CONCLUSIONS

In summary, we find that, independent of the specific initial surface conditions and independent of the method of As adsorption, the Si(110):As surface has a $\frac{2}{3}$-ML coverage with a particular, complex unit cell. We have shown theoretically that the ideally As-terminated Si(110) is not the lowest energy (110) surface and that corrugation can lead to preferred topologies. We have proposed a model for the reconstructed surface which is consistent with the As coverage and STM images and which contains no singly occupied dangling bonds. The structure consists of As atom chain segments in the top layer, substituted As atoms in the second-layer chains, and As adatoms bridging between second-layer chains.

ACKNOWLEDGMENTS

The work of J.E.N. and M.C.S. was supported in part by the U.S. ONR Contract No. N00014-92-C-0009.

[1]K. Takayanagi, Y. Tanishiro, M. Takahashi, and S. Takahashi, J. Vac. Sci. Technol. A **3**, 1502 (1985).

[2]R. D. Bringans, M. A. Olmstead, R. I. G. Uhrberg, and R. Z. Bachrach, Phys. Rev. B **36**, 9569 (1987); R. S. Becker, B. S. Swartzentruber, J. S. Vickers, M. S. Hybertsen, and S. G. Louie, Phys. Rev. Lett. **60**, 116 (1988); R. I. G. Uhrberg, R. D. Bringans, R. Z. Bachrach, and J. E. Northrup, *ibid.* **56**, 520 (1986).

[3]J. J. Lander and J. Morrison, J. Chem. Phys. **37**, 729 (1962).

[4]T. Arukawa, C. Y. Park, and S. Kono, Surf. Sci. **201**, L513 (1988); P. Martensson, G. Meyer, N. M. Amer, E. Kaxiras, and K. C. Pandey, Phys. Rev. B **42**, 7230 (1990).

[5]T. Takahashi, K. Izumi, T. Ishikawa, and S. Kikuta, Surf. Sci. **183**, L302 (1987); K. J. Wan, T. Guo, W. K. Ford, and J. C. Hermanson, Phys. Rev. B **44**, 3471 (1991).

[6]H. Ampo, S. Miura, K. Kato, Y. Ohkawa, and A. Tamura, Phys. Rev. B **34**, 2329 (1986).

[7]E. J. van Loenen, D. Dijkamp, and A. J. Hoeven, J. Microsc. **152**, 487 (1988).

[8]B. S. Krusor, D. K. Biegelsen, R. D. Yingling, and J. R. Abelson, J. Vac. Sci. Technol. B **7**, 129 (1989).

[9]W. Kohn and L. Sham, Phys. Rev. **140**, A1135 (1965).

[10]G. B. Bachelet and M. Schluter, Phys. Rev. B **25**, 2103 (1982).

[11]J. Ihm, A. Zunger, and M. L. Cohen, J. Phys. C **12**, 4409 (1979); M. T. Yin and M. L. Cohen, Phys. Rev. B **26**, 5668 (1982).

[12]A slightly higher energy for the Si(100)2×1:As surface may result in part from the elastic energy cost associated with forming the dimers.

[13]Chris Van de Walle (private communication).

[14]P. N. Keating, Phys. Rev. **145**, 637 (1966).

[15]J. Tersoff, Phys. Rev. B **43**, 9377 (1991).

[16]R. D. Meade and D. Vanderbilt, in *The 20th International Conference on the Physics of Semiconductors,* edited by E. M. Anatassakis and J. D. Joannopoulos (World Scientific, Singapore, 1990), p. 123.

[17]J. E. Northrup, in *The 18th International Conference on the Physics of Semiconductors,* edited by O. Engstrom (World Scientific, Singapore, 1986), p. 61.

[18]J. E. Northrup, Phys. Rev. B **44**, 1419 (1991).

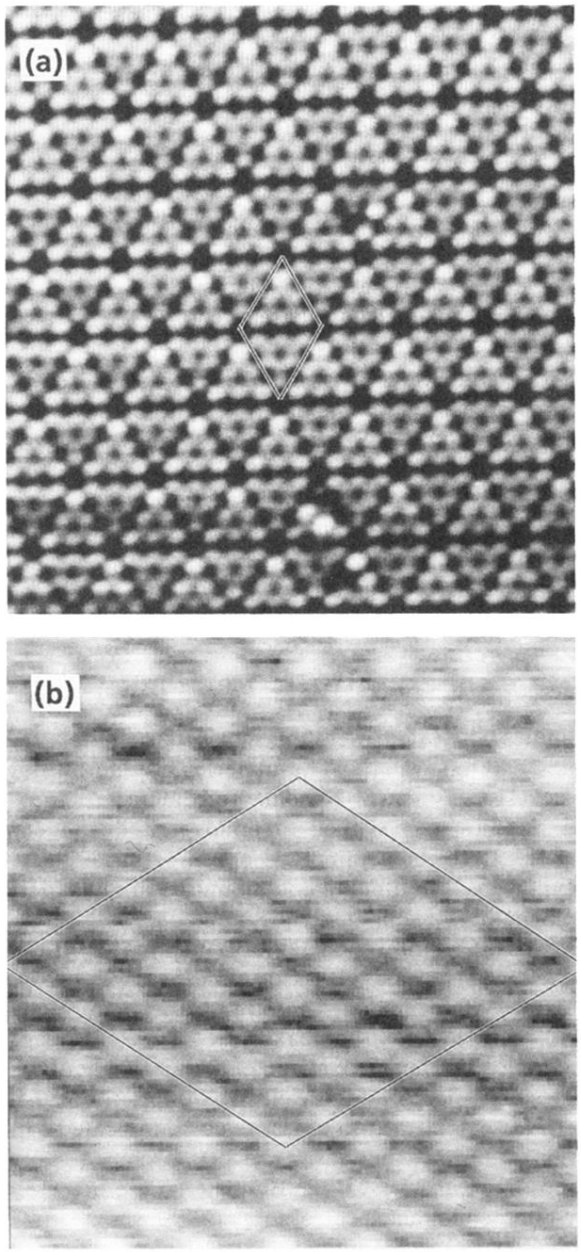

FIG. 1. Scanning tunneling microscope images of Si(111) surfaces. The sample bias was −2.0 V relative to the tip (filled states imaged) and demand current was 100 pA; (a) shows the (7×7) reconstruction of the bare surface and (b) shows the (1×1) As-terminated surface. Overlays indicate (7×7) cell size.

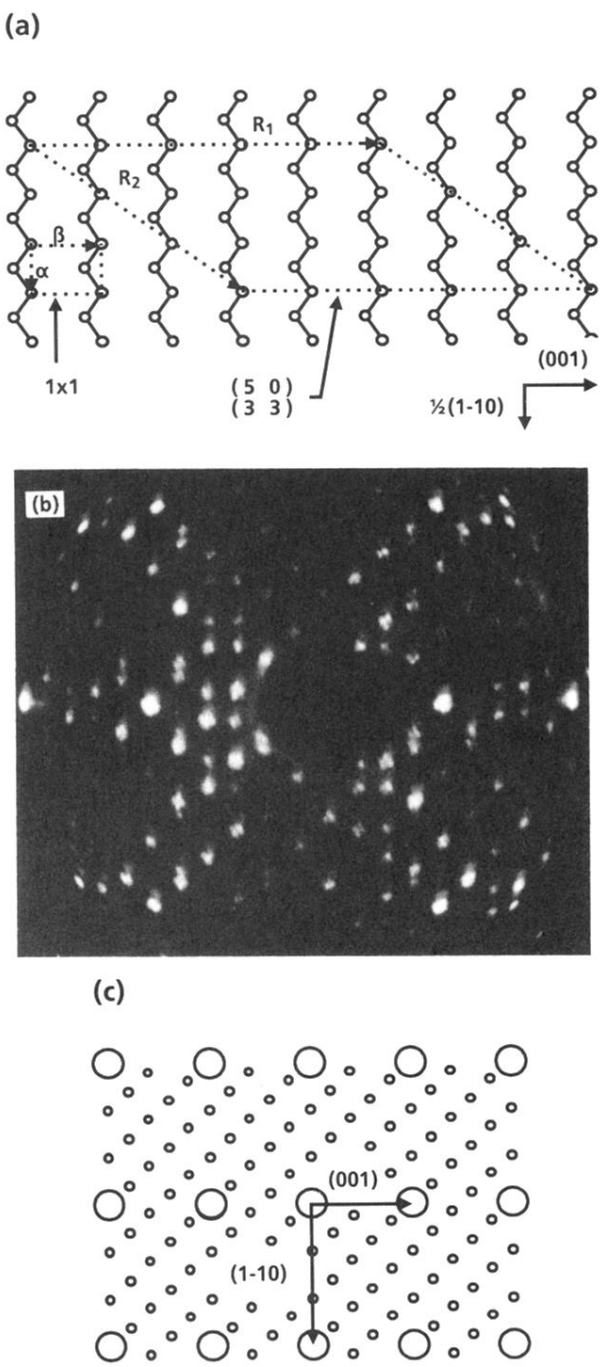

FIG. 2. (a) The ideally terminated Si(110) surface consisting of [1−10] chains of threefold-coordinated atoms. Overlays show a 1×1 cell for the ideal bare Si(110) surface and the real-space cell of the Si(110):As surface implied by the LEED results presented in (b) and (c); (b) LEED pattern from As-terminated Si(110) for $E=44$ eV; (c) inferred LEED spot pattern for single domain. Basis vectors are k-space conjugates corresponding to real-space directions [001] and [1−10].

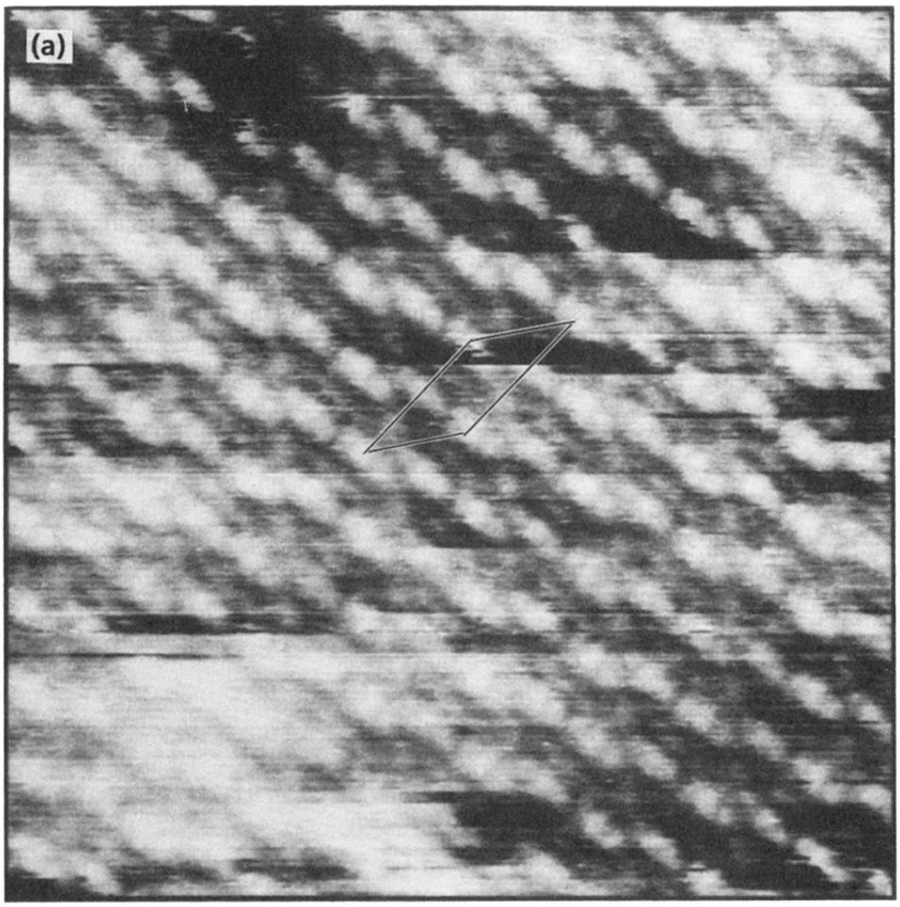

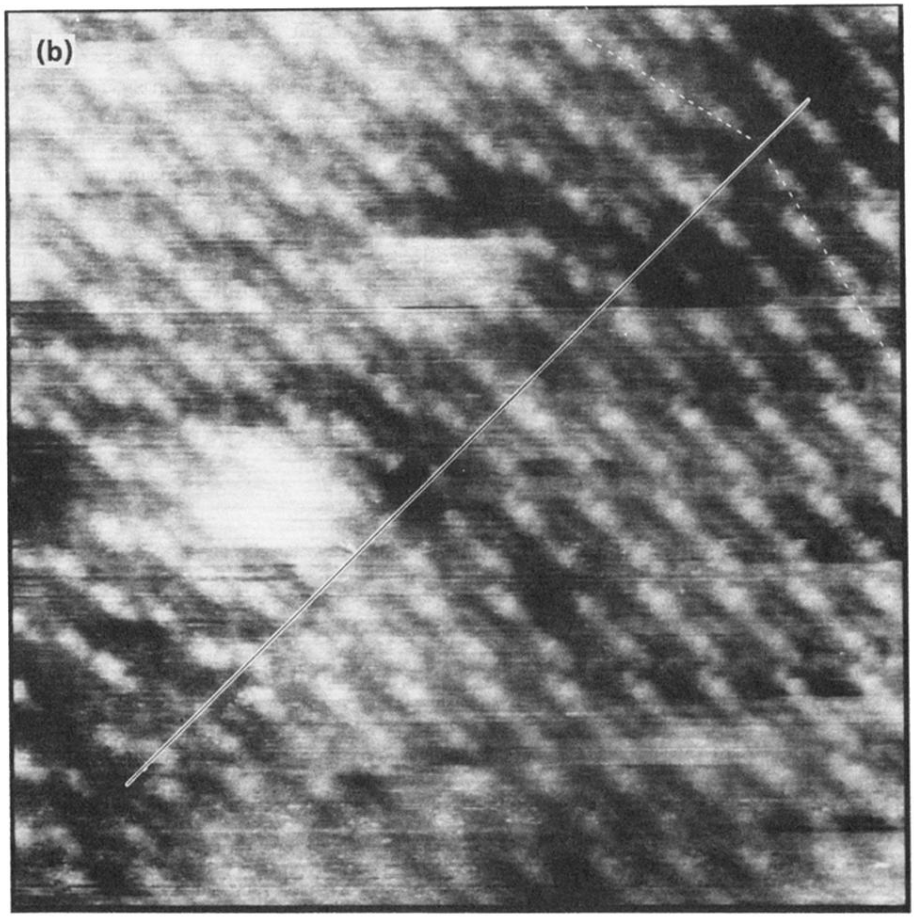

FIG. 3. STM images of Si(110) surface. Sample bias was −1.0 V relative to the tip. Demand current was 50 pA. (a) Typical gray scale image (where lightest represents highest above the surface) showing ordering of unit cells. Overlay indicates a unit cell as in Fig. 2(a). Image size is 16×16 nm. (b) Similar image including an antiphase reconstruction boundary. Image size is 18.5×18.5 nm.

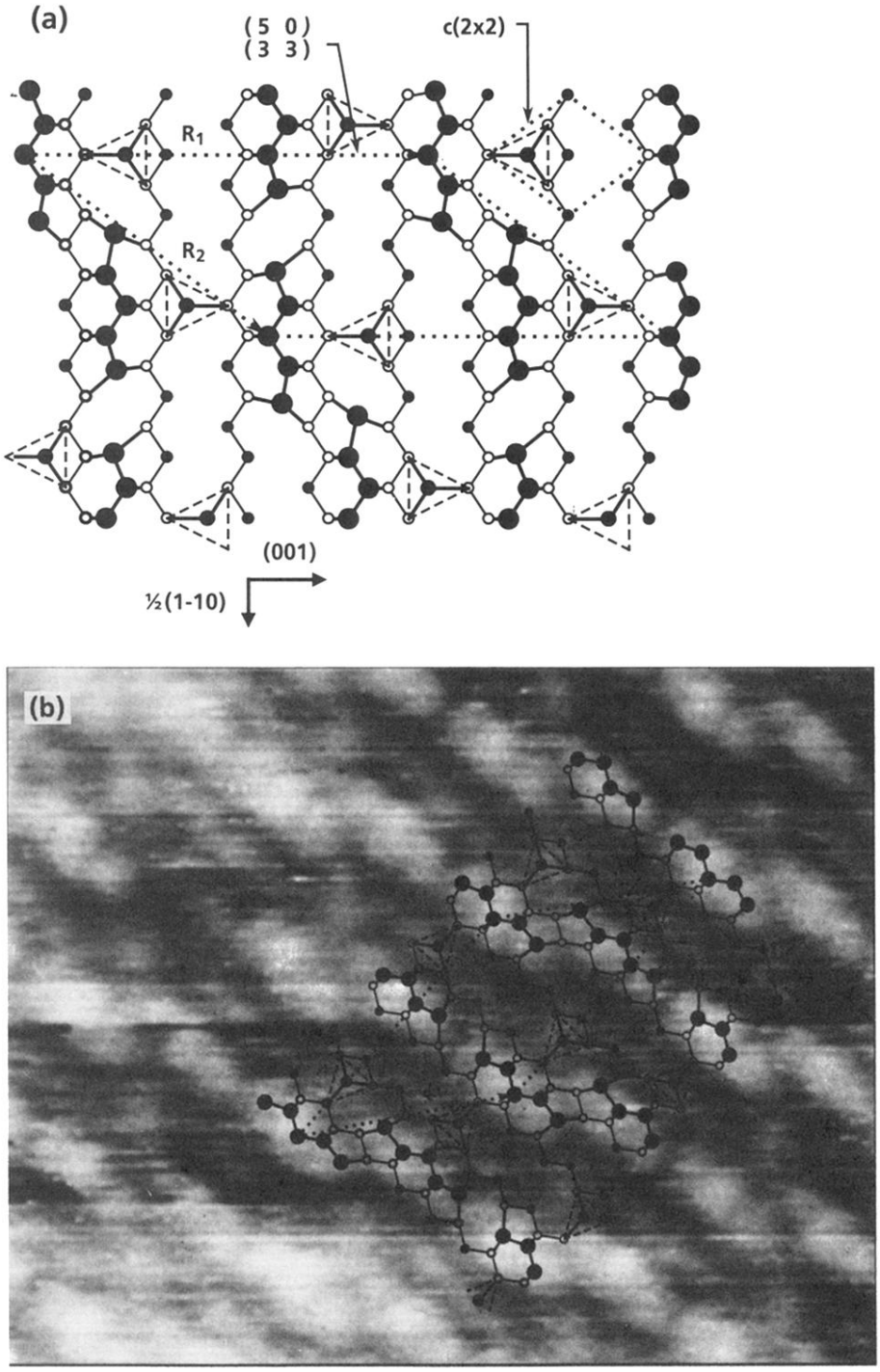

FIG. 4. (a) Ball and stick model of a $\frac{2}{3}$-ML As termination. Filled circles represent As atoms and empty circles represent Si. Largest filled circles lie in the top layer, intermediate sized circles represent the capping adatoms intermediate between layers, and the smallest filled circles represent substitutional As atoms in the lower layer. Dashed triangles are guides for the eye to mark adatom units. (b) Model superimposed on magnified region of Fig. 3(a). Image size is 6.5×8.5 nm.